

Numerical Simulation of Rock Breaking by Diamond Particles Under Ultra Deep Drilling Conditions

Zhongming Zhou^{1,2,*}

¹Sinopec Research Institute of Petroleum Engineering Co. Ltd., Beijing, 102206, China

²Sinopec Key Laboratory of Ultra-Deep Well Drilling Engineering, Beijing, 102206, China

*Corresponding author: Zhongming Zhou (e-mail: zhouzhm62054.sripe@sinopec.com).

Abstract: In the quest to access deeper fossil energy reserves, the past three decades have witnessed a concerted effort by scientists to develop and refine technologies capable of efficient drilling in environments characterized by high temperatures and pressures. Despite these advancements, our comprehension of the physical phenomena at play remains incomplete. A fundamental challenge pertains to the interaction between the rock and the drilling bit during drilling operations. This study delves into the influence of drilling bit pressure and rotation speed on the rock-breaking efficacy of impregnated diamonds under geostress conditions of 240 MPa and temperatures of 200°C. It juxtaposes these findings with those from rock-bit interaction experiments executed on a physical simulator, which was designed in accordance with similarity principles, in a controlled laboratory setting. Our findings indicate that for ultra-deep formations, a high Weight on Bit (WOB) coupled with a lower rotation speed results in enhanced rock cutting efficiency and a reduced rate of bit wear. Consequently, we recommend optimal drilling parameters of 8.0 to 8.5 kN for WOB and a rotational speed range of 180 to 240 rad/min. Furthermore, the study underscores the profound impact of horizontal differential stress on the rate of penetration (ROP). The insights gleaned from these tests are instrumental in refining the design of rock-breaking tools and optimizing drilling parameters, thereby augmenting the efficiency of rock breaking in challenging drilling environments.

Keywords: Ultra-deep Well, Similarity Principle, Drilling Parameter Optimization, Rock-bit Interaction.

1. Introduction

Over the last three decades, researchers have made certain research achievements in the methods and theories of efficient rock breaking under deep and ultra deep geological conditions. Despite these advancements, gaps remain in our comprehensive understanding of the physical phenomena that manifest during the cutting process. The mechanisms underlying the failure, fracture, or fragmentation of rock by mechanical tools has been extensively studied by means of theoretical analyses, experiments and numerical simulations [1-2].

Typically, the primary objective of both experimental and numerical research is to validate the accuracy of theoretical models. Conducting physical tests on rocks within a controlled environment is a relatively straightforward endeavor, and the outcomes of such tests are generally readily accepted. However, these results are subject to significant variability, largely due to random factors, most notably the inherent heterogeneity of natural materials. To mitigate the impact of these random elements, a substantial number of repeat tests are necessary. This requirement often results in high costs, yet the yield of substantial research findings remains somewhat limited. Moreover, researchers are generally constrained to utilizing conventional measurement equipment and experimental methods. Such tools primarily facilitate the acquisition of insights pertaining to the final stages of the process, leaving the details of the crushing process largely obscure, as noted by Kou et al and Xie Q et al [3-4]. In contrast, numerical modeling typically yields reliable results under specified conditions. Despite often incorporating certain critical simplifications, it offers valuable visualizations of the

crushing process, which can be instrumental in understanding these phenomena. Therefore, the integration of numerical simulation and physical testing methodologies has emerged as an ideal approach for research in this field.

Numerical modeling plays a pivotal role in simulating the rock breaking process during drilling, offering reliable results under specific conditions and facilitating insightful visualization of this complex process. In the analysis of drilling rock breaking, several numerical methods are prominently employed, such as the finite difference method (FDM), finite element method (FEM), boundary element method (BEM) and discrete element method (DEM) [5-7]. The FEM is particularly notable for its applicability and adaptability, especially when simulating materials characterized by heterogeneity, nonlinearity, and complex boundary conditions. Moreover, the FEM has emerged as the most extensively utilized numerical calculation method in contemporary engineering analysis, encompassing fields such as rock mechanics and geotechnical engineering[8]. Its widespread adoption is attributed to its versatility in handling a variety of challenges. These include managing material heterogeneity, addressing nonlinear deformations (predominantly plasticity), dealing with intricate boundary conditions, solving dynamic problems, and effectively simulating complex constitutive models and even fracturing phenomena. Due to these capabilities, FEM is highly regarded and extensively utilized within the engineering and technical communities.

When seeking the most effective continuum method for simulation, the FEM stands out as the most reliable for simulating the rock breaking process during bit drilling. However, a notable limitation in most existing research reports employing FEM for this purpose is the omission of

high temperature and high pressure geological conditions. This oversight often leads to significant discrepancies between the numerical simulation results and the actual conditions encountered in ultra-deep drilling sites. To bridge this gap, an ideal approach involves the integration of numerical simulations with physical tests. This combined methodology enables the validation of rock-drill interaction models under the specific conditions of ultra-deep triaxial geostress. By assessing rock breaking efficiency and optimizing drilling parameters, a theoretical model of the ROP for ultra-deep drilling test simulations can be established, based on similarity theory. Furthermore, the research on rock breaking mechanism of impregnated diamond bit is conducive to scientific and reasonable selection of drilling parameters and optimization evaluation of bit structures. Such advancements not only improve operational effectiveness but also help in adapting to the challenging conditions of ultra-deep drilling environments.

2. Establishment of numerical model

A. Geometry and grid design

The finite element model, comprising diamond grains and a granite rock mass structure, was meticulously meshed using Hypermesh, and subsequent stages involving load setting, calculation analysis, and post-processing were conducted utilizing ABAQUS. Figure 1a illustrates the comprehensive finite element model of the diamond grain rock breaking structure, with its geometric dimensions delineated as follows: the simulated granite plane measures 100 mm × 100 mm, with a thickness of 12 mm. The model includes a diamond particle represented as a regular hexahedron, each side measuring 2 mm. For the granite structure, a three-dimensional reduced integral solid element was employed, with a unit size of 1 mm. This choice is particularly advantageous for its ability to avert shear self-locking and its suitability for analyzing large deformation issues.

The simulation of the diamond particle model, as depicted in Figure 1c, was achieved through the utilization of three-dimensional six-node solid units, maintaining a consistent unit size of 1 mm. The trajectory of the diamond particles is defined as follows: originating from the center of the upper surface of the simulated granite, a circular motion with a radius of 25 mm is executed. To enhance clarity and quantification of the rock breaking process by diamond particles, a densification of the grid along the diamond particle trajectory was implemented, as shown in Figure 1b. This densification entailed establishing a 4 mm wide cutting zone, located 2 mm on either side of the rotational path, followed by an encryption process. The transition area, bridging the densified and non-densified grids, employs a pentahedron-to-hexahedron grid transition for accommodating large size variations, with the mesh size in the densified contact area reduced to 0.5 mm.

B. Parameter selection of structural constitutive model

The constitutive model of the structure under consideration is characterized by a set of critical parameters of granite, which are measured at 240 MPa and 200 °C in previous published articles[9]. These parameters include a density of 2.80 g/cm³, Young's modulus of 23.91 GPa, and a Poisson's ratio of 0.105, with the compressive strength recorded at 453.10 MPa. For the simulation of plasticity, the modified Drucker-Prager constitutive model is employed, which characterizes the material as exhibiting yield characteristics that are pressure-dependent, namely, an increase in material

strength concurrent with rising pressure. Compared with Mohr-Coulomb model, this constitutive model considers deviatoric stress as the criterion of material failure, reflecting the enhanced strength characteristics during diamond particle rock breaking, as well as the influence of volumetric stress on the strength of granite.

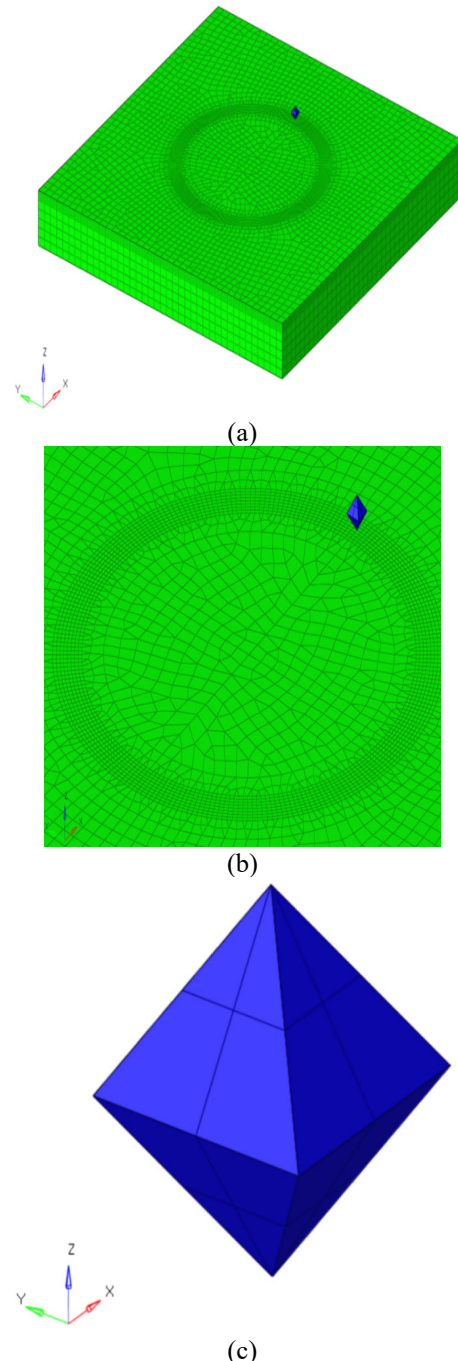


Figure 1. Geometry and grid design diagram of the model. (a) Numerical simulation of rock fragmentation by diamond particles. Granular diamond particles (blue) interact with a granite sample (green), inducing a 4 mm densified zone along the rotating track; (b) Numerical grid setup in operation track area; (c) Diamond particle model.

The modified Drucker-Prager model has been frequently utilized in studies focusing on rock shear failure, as evidenced in the works of Jia Yanjie and Zhu Xiaohua[10-11], underscoring its applicability and effectiveness in capturing

the complexities of rock behavior under stress. According to the modified Drucker-Prager model, the effect of intermediate principal stress (σ_2) on the rock breaking process is duly considered. This effect is articulated through the normal stresses (σ_{oct}) and (τ_{oct}) on the octahedral plane, that is:

$$\tau_{oct} = \tau_0 + m\sigma_{oct} \quad (1)$$

The normal stress σ_{oct} can be expressed as:

$$\sigma_{oct} = \frac{1}{3}(\sigma_1 + \sigma_2 + \sigma_3) \quad (2)$$

Shear stress τ_{oct} can be expressed as:

$$\tau_{oct} = \frac{1}{3}\sqrt{(\sigma_1 - \sigma_2)^2 + (\sigma_2 - \sigma_3)^2 + (\sigma_3 - \sigma_1)^2} \quad (3)$$

Where σ_1 , σ_2 and σ_3 are the maximum principal stress, intermediate principal stress and minimum principal stress of rock respectively. τ_0 can be expressed as:

$$\tau_0 = -\frac{\sqrt{6}}{3}k \quad (4)$$

Where m can be expressed as $m = -\sqrt{6}\alpha$, k and α are parameters corresponding to the cohesion (C) and friction angle (ξ) of the rock, respectively.

Therefore, the Drucker-Prager constitutive model of granite needs parameters such as friction angle, expansion angle, stress ratio and enhanced compressive stress (or tensile stress). The model stipulates a friction angle of 34° and an expansion angle of 15° . Additionally, the ratio of triaxial tensile strength to triaxial compressive strength, known as the Flow Stress Ratio, is determined to be 0.8, as documented in the research by Peng Xu et al. [12]. The failure parameter of the structure is shear failure. This criterion is particularly relevant to the failure mode observed when the drilling bit interacts with the rock, manifesting predominantly as a squeezing effect in this study. The essential parameters for this failure mode include fracture strain, shear stress ratio, and strain rate. In the current model, the fracture strain is set at 0.02, with a corresponding shear stress ratio and strain rate of 0.02. Since the possibility of failure of the impregnated diamond bit during the cutting process is not a primary consideration, diamond particles are treated as rigid bodies in the model. The detailed parameters for the granite sample model are systematically outlined in Table 1.

Table 1. Specific Setting Parameters of Granite Sample Model

Quantity	Unit	Value
Density	g/cm ³	2.80
Young's modulus	GPa	23.91
Poisson's ratio	/	0.105
Compressive strength	MPa	453.10
Friction angle	°	34
Expansion angle	°	15
Flow stress ratio	/	0.8
Failure displacement	/	0.02

C. Structural Analysis Step Settings

In previously published studies[9], the parameters for an ultra-deep drilling simulator were derived based on the

similarity principle. The lip diameter of the impregnated diamond bit used in these simulations is reported to be 50.8 mm, and the contact area between a single diamond particle and rock is assumed to correspond to the maximum cross-sectional area of the interaction. Subsequently, the forces applied to the bit, adhering to the similarity principle, are calculated to be 5 kN, 6.5 kN, 7.19 kN, and 9.38 kN. Furthermore, the pressures exerted on the simulated diamond particles are determined by converting these values according to the area ratio. This results in pressures of 102 N, 122 N, 147 N, and 191 N, respectively.

The structural analysis requires consideration of geometric large deformation and high strain rate, thus necessitating the use of explicit dynamic analysis. In this context, the analysis time corresponds to real-time. For instance, based on the calculation example, when the rotational speeds are set at 170 rad/min, 220 rad/min, 270 rad/min, and 320 rad/min, the respective running times for one revolution are calculated to be 0.037 s, 0.0286 s, 0.0233 s, and 0.0196 s. In setting up the analysis steps, it is crucial to account for the unit damage caused by cutting. Additionally, appropriate selections should be made in the status output to ensure the relevant data is captured and analyzed effectively.

D. Boundary and load condition setting

In the configuration of constraint coupling for the model, measures are taken to ensure smooth operation of the drilling bit, preventing any overturning or unintended displacements during the cutting process. The model employs the center of the drilling bit as the control point for setting constraint coupling, as illustrated in Figure 2a. This setup effectively restricts the degrees of freedom for all points on the drilling bit, thereby stabilizing its movement.

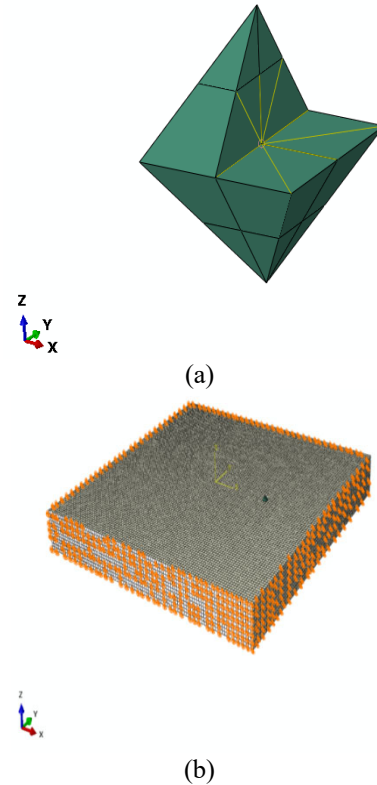


Figure 2. Boundary and load condition setting. (a) Constraint coupling setting interface (All four directions are constrained except the horizontal X and Y directions); (b) Boundary condition setting (Yellow mark is the constraint boundary of rock sample).

Regarding the boundary settings, they include fixed constraints around the rock, depicted in Figure 2b. These constraints specifically address the three translational degrees of freedom at the constraint node. Additionally, settings encompass the drill center point, restricting its out-of-plane degrees of freedom and rotational degrees of freedom, to maintain consistent cutting action.

In terms of load condition settings, since the diamond particle is considered a rigid body in the model, it precludes the possibility of assigning a separate reference point for rotational speed loading. Therefore, the linear velocity is decomposed as follows:

$$V_x = V_0 * \sin \theta \quad (5)$$

$$V_y = V_0 * \cos \theta \quad (6)$$

$$V_0 = w * R \quad (7)$$

Where V_0 is the linear velocity, w is the angular velocity, and R is the radius of rotation. For points on the circumference, geometric parameters can be substituted to compute the relevant rotation angle. Subsequently, the velocity component at a given angle can be determined and applied using a definition table.

E. Model validation

Building upon the granite parameters established in previous study [9] for simulating rock breaking by diamond particles, the same simulation methodology is applied to conduct a numerical simulation of granite under triaxial compression. This is done to validate the reliability of the diamond particle rock breaking simulation under the predetermined granite parameters. Figure 3 presents the triaxial compression finite element model of granite. The simulated granite sample is modeled with a height of 100 mm and a diameter of 50 mm. The geometric layout, grid design, and structural constitutive model parameters are consistent with those used for a portion of the granite models discussed in Section 2.1 of this paper. The model features a unit size of 5 mm, comprising 2562 units and 3047 nodes. The lower end of the rock sample is fixed and constrained.

In accordance with previously published articles, a confining pressure of 240 MPa is radially applied to the rock, and the temperature field of the granite sample is set at 200 °C. The upper end of the simulated granite sample is treated as an analytical rigid body pressing plate, as referenced in Zhu Xiaohua et al. (2019). The axial movement rate of this pressing plate is aligned with the physical simulation parameters adopted in Section 2.3 of this paper.

Figure 3 illustrates a comparison of the stress-strain curves obtained from both physical and numerical simulations of triaxial compression of rocks under a confining pressure of 240 MPa and a temperature of 200 °C. Additionally, Figure 4 compares the morphology of granite post-triaxial compression failure as observed in both physical and numerical simulations at the same conditions. From the observations in Figure 5a and Figure 5b, it is evident that the numerical simulation results accurately reflect the failure mode and stress-strain curve characteristics of granite, showing strong congruence with the results of indoor tests. This alignment indicates that the numerical simulation model of diamond particle rock breaking under the specific conditions of a confining pressure of 240 MPa and a temperature of 200 °C is indeed reliable.

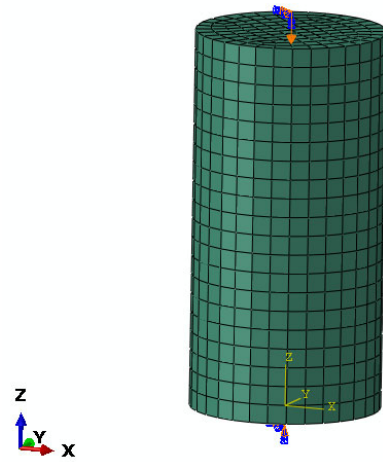


Figure 3. Triaxial compression finite element model of granite

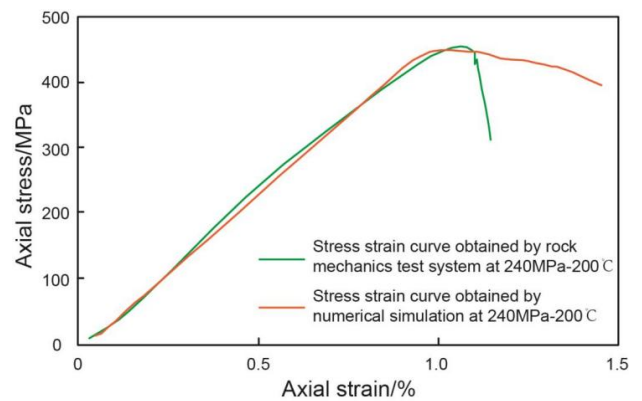


Figure 4. Comparison of stress-strain curves between physical test and numerical simulation of triaxial compression of rocks under a confining pressure of 240 MPa and a temperature of 200 °C

3. Establishment of Numerical Model

The rock-breaking mechanism of an impregnated diamond bit operates through micro-cutting, facilitated by diamond particles distributed along the bit's lip, which engage the rock as the bit rotates. The performance of an impregnated diamond bit in engineering applications is influenced by several critical factors. These include the concentration and size of diamond particles on the tread, the wear resistance of the cemented carbide that coats these diamond particles, the retention force of the diamond particles, and the degree of compatibility between the drilling process parameters and the geological strata being drilled.

During the rock-breaking process, the wear pattern of the impregnated diamond bit unfolds as follows: when the tread of the bit makes contact with the rock, the rotation of the bit causes the diamonds to protrude from the edge. Subsequently, these diamond particles undergo wear, breakage, and detachment due to the interaction between the rock and the drilling bit. Simultaneously, the cemented carbide layer is also worn away by the rock, until new diamond particles emerge to continue the rock-breaking process. This cycle repeats until the impregnated diamond bit becomes ineffective and is ultimately discarded. Therefore, for the purpose of simplifying the study and facilitating numerical computation, the rock-breaking process of the impregnated diamond bit is modeled as the simulation of a single diamond particle breaking rock, deliberately omitting the impact of diamond

particle shedding. This approach streamlines the factors influencing the research subject and aids in the efficient execution of numerical calculations.

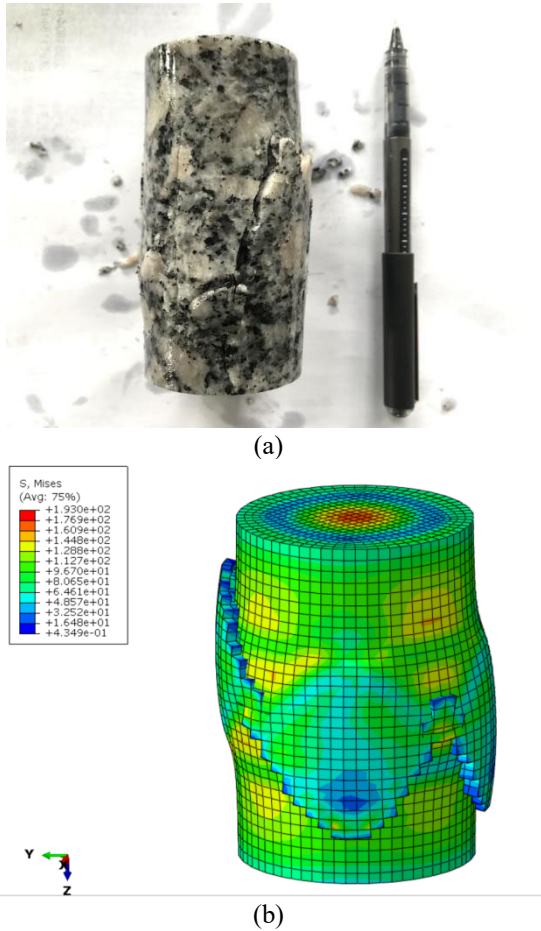


Figure 5. Comparison of granite morphology after triaxial compression failure obtained by physical test and numerical simulation under a confining pressure of 240 MPa and a temperature of 200 °C

Table 2 shows the numerical simulation experimental parameters for single diamond particle rock breaking. This simulation critically assesses the principal factors influencing the efficiency of rock breaking when conducted by an impregnated diamond particle. In conjunction with the physical simulations of rock breaking using an impregnated diamond bit, as documented in prior scholarly articles [9], this approach facilitates the validation of drilling efficiency and the observed trends in bit wear during physical simulation tests under ultra-deep formation conditions. Moreover, this integrated methodology effectively demonstrates the research's validity regarding the impacts of varying stress conditions on bit footage. It contributes both test data and analytical support for the development of a theoretical ROP model tailored for ultra-deep drilling simulations. This model is grounded in the principles of similarity theory, offering a robust framework for understanding and optimizing drilling performance under diverse geological stresses. The rock-breaking mechanism of an impregnated diamond bit operates through micro-cutting, facilitated by diamond particles

distributed along the bit's lip, which engage the rock as the bit rotates. The performance of an impregnated diamond bit in engineering applications is influenced by several critical factors. These include the concentration and size of diamond particles on the tread, the wear resistance of the cemented carbide that coats these diamond particles, the retention force of the diamond particles, and the degree of compatibility between the drilling process parameters and the geological strata being drilled.

Table 2. Numerical simulation scheme of rock breaking by single diamond particle

Model code	Angular velocity rad/min	Vertical force N
A1	170	102
A2		122
A3		147
A4		191
B1	220	102
B2		122
B3		147
B4		191
C1	270	102
C2		122
C3		147
C4		191
D1	320	102
D2		122
D3		147
D4		191

Figure 6 serves as an illustrative example, depicting the variations in equivalent stress and equivalent plastic strain of diamond particles at different cutting positions. These variations are determined through simulations that incorporate a combination of 16 different rotating speeds and WOB settings as listed in Table 2. The simulation's objective is to analyze the pattern of rock breaking footage changes of impregnated diamond bits under varying conditions. In this study, the focus is on calculating the plastic dissipation energy of the rock subjected to different rotating speeds and bit pressures. Plastic dissipation energy is a key indicator of the extent of plastic shear failure. It provides a metric for gauging the rock breaking efficiency, or footage efficiency, of impregnated diamond bits, as highlighted in the work of He M et al. [13].

Figure 7a, Figure 7b, Figure 7c, and Figure 7d present a comprehensive summary of the relationship between the plastic dissipation energy exerted by diamond particles on rocks under various WOB conditions over time, at rotational speeds of 170 rad/min, 220 r/min, 270 rad/min, and 320 rad/min, respectively. To present these relationships in a more intuitive and visually striking manner, a three-dimensional representation of the correlation between the rotational speed of diamond particles, WOB, and the plastic dissipation energy of rocks in numerical simulation is illustrated in Figure 8. These visualizations are instrumental in understanding the dynamics of rock breaking in relation to the operational parameters of the impregnated diamond bits.

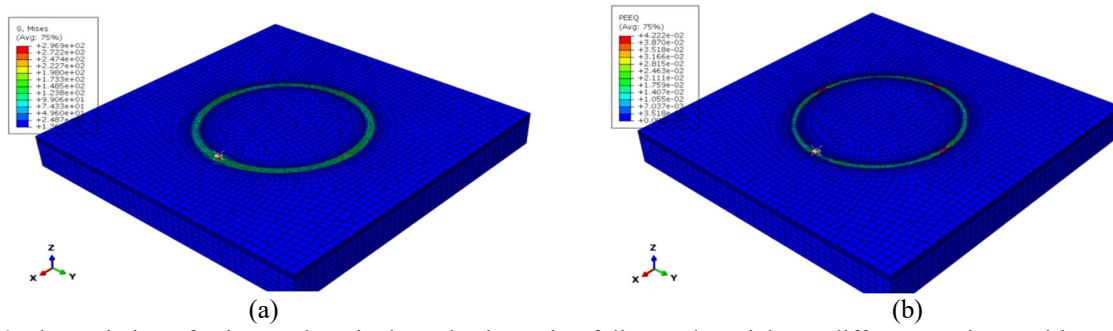


Figure 6. The variation of Mises and equivalent plastic strain of diamond particles at different cutting positions when rotating speed is 270 rad/min and WOB is 147 N. (a) Equivalent stress variation of diamond particles at different cutting positions; (b) Equivalent plastic strain variation of diamond particles at different cutting positions.

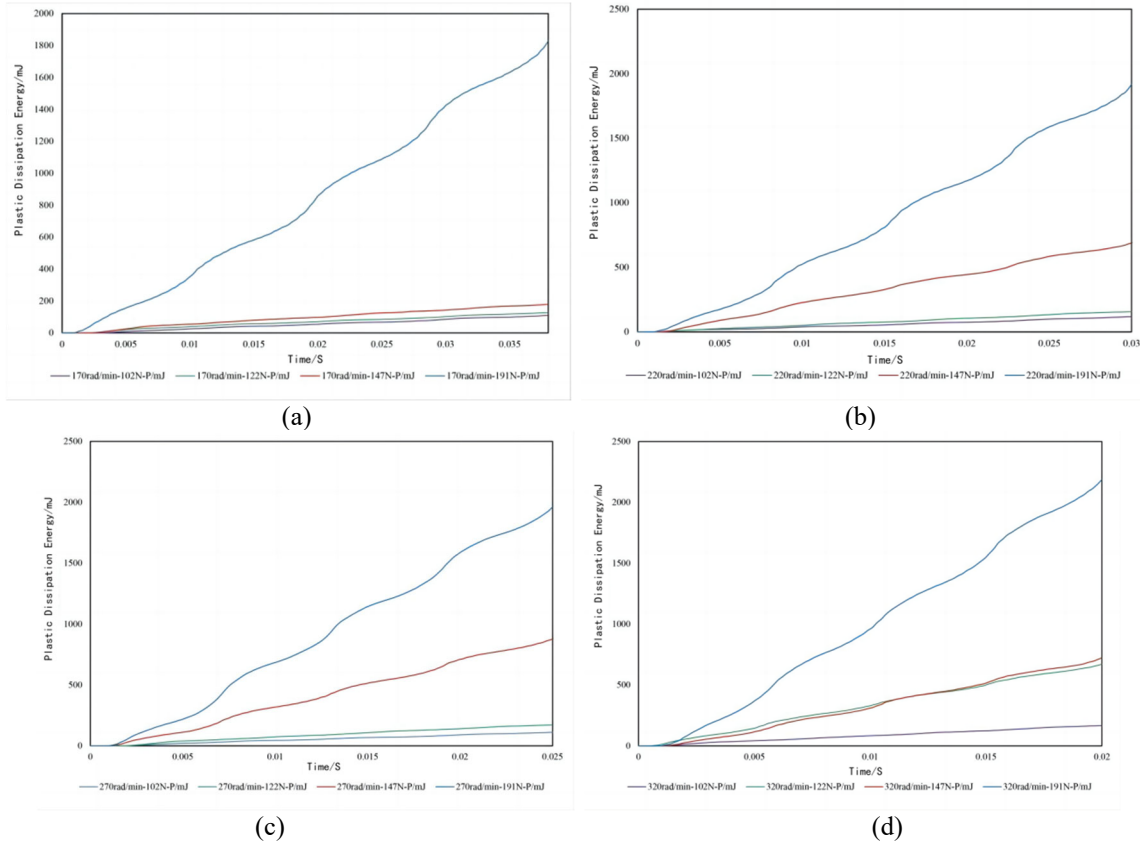


Figure 7. The time-dependent relationship of plastic dissipation energy of diamond particles applied to rocks under different WOB conditions. (a) The variation of diamond particles on the plastic dissipation energy of rock under different WOB conditions (rotating speed $v=170$ rad/min); (b) The variation of diamond particles on the plastic dissipation energy of rock under different WOB conditions (rotating speed $v=220$ rad/min); (c) The variation of diamond particles on the plastic dissipation energy of rock under different WOB conditions (rotating speed $v=270$ rad/min); (d) The variation of diamond particles on the plastic dissipation energy of rock under different WOB conditions (rotating speed $v=320$ rad/min).

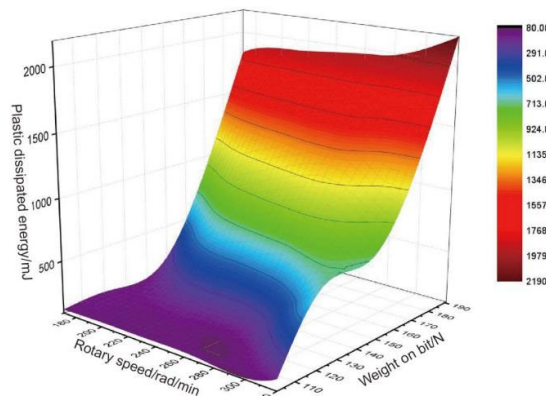


Figure 8. The Relationship between rotational speed, WOB and plastic dissipation energy of diamond particles

This paper extends its investigation to the evaluation of rock-breaking wear of impregnated diamond bits under various rotating speeds and WOB conditions, simulating an ultra-deep geological environment. A key focus is on assessing the wear of diamond particles, which is characterized by the cutting force exerted by these particles on granite. This cutting force is determined as the resultant

force of the rock's reaction in the horizontal directions (FX and FY) during the rock-breaking process by diamond particles. Mathematically, the cutting force F is calculated as:

$$F = \sqrt{F_x^2 + F_y^2} \quad (8)$$

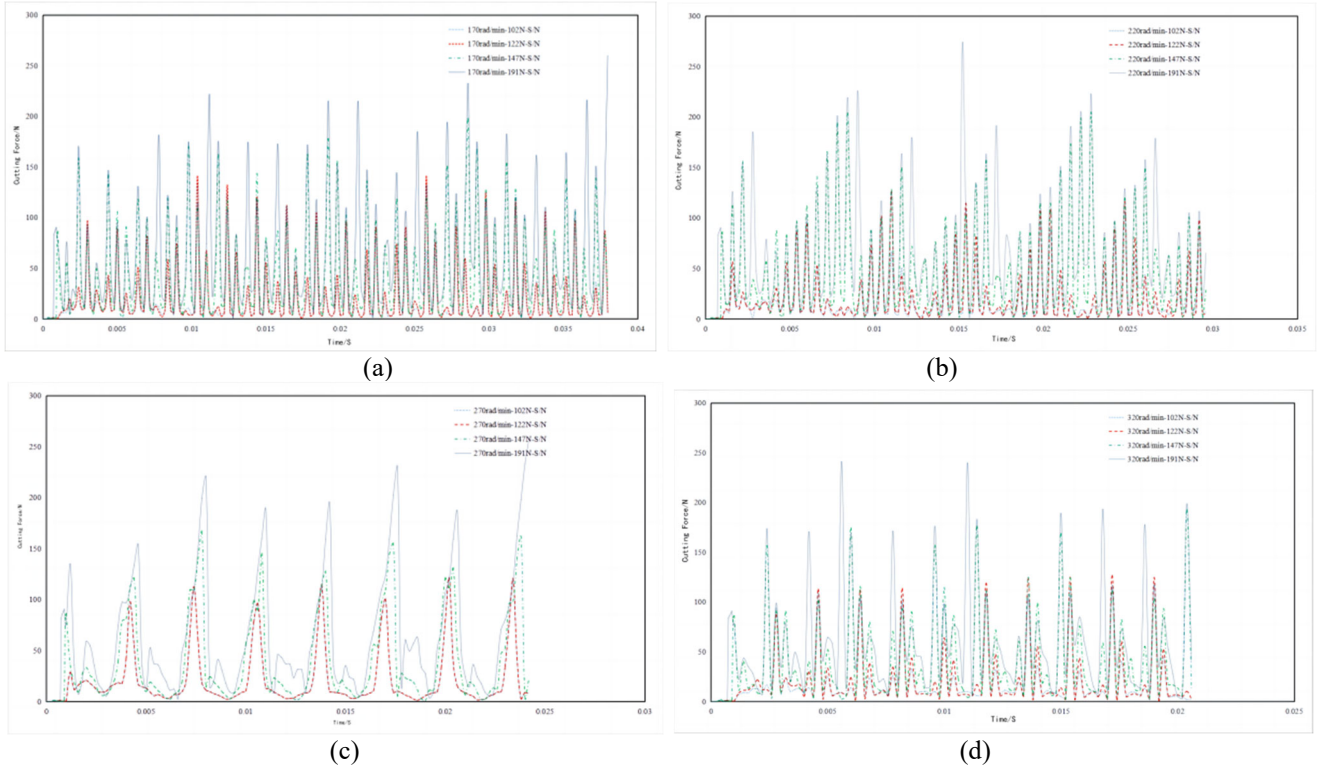


Figure 9. The time-dependent relationship of temporal variation of rock cutting force on diamond particles applied to rocks under different WOB conditions. (a) The variation of cutting forces on rock surfaces under different WOB conditions (rotating speed $v=170$ rad/min); (b) The variation of cutting forces on rock surfaces under different WOB conditions (rotating speed $v=220$ rad/min); (c) The variation of cutting forces on rock surfaces under different WOB conditions (rotating speed $v=270$ rad/min); (d) The variation of cutting forces on rock surfaces under different WOB conditions (rotating speed $v=320$ rad/min).

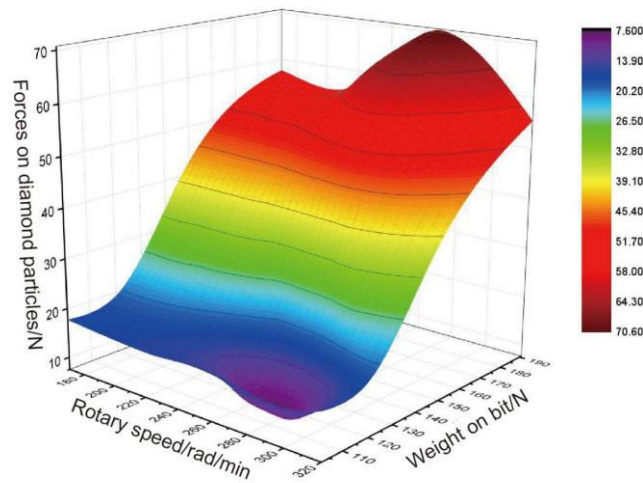


Figure 10. The relationship among diamond particle rotation speed, WOB and cutting force.

Figure 9a, Figure 9b, Figure 9c, and Figure 9d display the simulation summaries of the changes in rock cutting force over time under different WOB conditions for diamond particles at rotational speeds of 170 rad/min, 220 rad/min, 270 rad/min, and 320 rad/min, respectively. These figures

collectively illustrate that the forces exerted by diamond particles during rock breaking are periodic in nature. This periodicity encompasses a process of contact, crack initiation, inoculation, and destruction. To provide a more intuitive and vivid depiction of the relationship between diamond particle

speed, WOB, and cutting force in the numerical simulation, a three-dimensional image has been created (Figure 10).

The numerical simulation of the diamond rock-breaking process offers insightful analysis into how the speed of diamond particles and bit pressure influence the cutting force exerted by diamond particles and the dissipation energy of the rock. From the data illustrated in Figure 10, it is observed that when the WOB is relatively low (ranging between 102 and 122 N), the rock's dissipation energy remains minimal. This trend aligns closely with the outcomes observed in indoor physical simulation tests, particularly when the WOB ranges between 5 and 6.5 kN.

Further insights gained from Figure 10 reveal that as the rotational speed of diamond particles escalates beyond a certain threshold (exceeding 260 rad/min), there is a marked increase in the force exerted on the diamond particles. This phenomenon indicates a reduction in cutting efficiency and an escalation in the wear rate of the bit as the bit weight increases. Consequently, it becomes imperative to identify the optimal WOB value and rotational speed that strike a balance between high cutting efficiency and low wear rate. Comparing the findings from Figure 8 and Figure 10, it is deduced that under ground stress conditions of 240 MPa and a temperature of 200 °C, the optimal drilling parameters are a WOB of 150 to 170 N and a rotational speed of 220 to 240 rad/min. Notably, these parameters are in close agreement with the optimal drilling parameters identified through indoor physical simulation tests.

4. Conclusions

This study employs finite element numerical simulations to analyze the diamond rock-breaking process, with a specific focus on the influence of diamond particle velocity and bit pressure on cutting forces exerted by the diamond particles and the energy dissipated within the rock. The objective is to pinpoint the primary factors that affect the efficiency of breaking rock masses using impregnated diamond particles. To strengthen the credibility of our research, we draw comparisons with physical simulations of rock breaking utilizing impregnated diamond bits, as detailed in previously published works. This comparative analysis verifies the robustness of our findings, particularly concerning drilling efficiency, bit wear, and the consequences of varying stress conditions on bit performance within ultra-deep geological formations. As a result, this study provides substantial empirical and data-based support for the development of a theoretical ROP model tailored for ultra-deep drilling simulations, grounded in the principles of similarity theory. The key discoveries from our research include:

(1) Acknowledging the significant impact of high temperature and high geostress on rock-breaking efficiency, the study successfully simulates the rock-breaking process by diamond particles under ultra-deep drilling conditions, utilizing the principles of similarity theory.

(2) The results of the numerical simulation, which include the assessment of diamond particle cutting force and rock plastic dissipation energy under high-temperature and high-pressure conditions, effectively illustrate the trend of bit weight and rotation speed on the rock-breaking efficiency of impregnated diamond bits. Furthermore, these results indicate that the optimal mechanical parameters for drilling are a WOB of 8.0 to 8.5 kN and a rotational speed of 180 to 240 rad/min. Under these optimal conditions, a higher ROP and lower bit wear are attainable.

(3) The numerical simulation outcomes, specifically the measurements of cutting force and plastic dissipation energy under extreme temperature and pressure conditions, confirm the reliability of physical simulation tests' findings in terms of drilling efficiency and bit wear under ultra-deep formation conditions. Additionally, these results support the investigation into how varying stress conditions affect bit footage, thus providing crucial experimental validation and data support for establishing a theoretical model of ROP for ultra-deep drilling simulations based on similarity theory.

Acknowledgment

The work was supported by the research project of the Ministry of Science and Technology of Sinopec (Fine Description of Geological Factors in Ultra Deep Drilling and Drilling Optimization Design Technology, No. P21081-1), by the research project of the Ministry of Science and Technology of Sinopec (Study on the Mechanical Properties of Carbonate Rocks in Ultra High Temperature and High Pressure Formations, No. P23038).

References

- [1] D. D. K. Wayo, S. Irawan, A. Satyanaga et al., "Modelling and Simulating Eulerian Venturi Effect of SBM to Increase the Rate of Penetration with Roller Cone Drilling Bit," *Energies*, vol. 16, no. 10, pp. 4185, 2023.
- [2] X. Zhang, X. Huang, S. Qi et al., "Numerical Simulation on Shale Fragmentation by a PDC Cutter Based on the Discrete Element Method," *Energies*, vol. 16, no. 2, pp. 965, 2023.
- [3] S. Kou, H. Kiu, P. A. Lindqvist et al., "Rock fragmentation mechanisms induced by a drill bit," *International Journal of Rock Mechanics and Mining Sciences*, vol. 41, Suppl. 1, pp. 527-532, 2004.
- [4] Q. Xie, C. Zhong, D. Liu et al., "Operation Analysis of a SAG Mill under Different Conditions Based on DEM and Breakage Energy Method," *Energies*, vol. 13, 2020. DOI:10.3390/en13205247.
- [5] W. G. P. Kumari, P. G. Ranjith, M. S. A. Perera et al., "Hydraulic fracturing under high temperature and pressure conditions with micro CT applications: geothermal energy from hot dry rocks," *Fuel*, vol. 230, pp. 138-154, 2018.
- [6] W. Liu, X. Zhu, J. Jing, "The analysis of ductile-brittle failure mode transition in rock cutting," *Journal of Petroleum Science and Engineering*, vol. 163, pp. 311-319, 2018.
- [7] A. Z. Mazen, N. Rahmanian, I. M. Mujtaba et al., "Effective mechanical specific energy: A new approach for evaluating PDC bit performance and cutters wear," *Journal of Petroleum Science and Engineering*, vol. 196, 108030, 2021.
- [8] N. H. Adli, I. Namgung, "An Investigation of Structural Strength of Nuclear Fuel Spacer Grid," *Energies*, vol. 17, no. 2, pp. 458, 2024.
- [9] Z. Zhou, S. Li, X. Li et al., "Evaluation of rock-bit interaction test under simulated ultra-deep well conditions based on similarity principle," *Journal of Petroleum Science & Engineering*, no. 211, art. no. 211, 2022.
- [10] Yan-jie Jia, Ping Jiang, Hua Tong, "3D mechanical modeling of soil orthogonal cutting under a single reamer cutter based on Drucker-Prager criterion," *Rock and Soil Mechanics*, vol. 34, no. 5, pp. 1429-1436, 2013.
- [11] Xiaohua Zhu, Zhaowang Dan, "Numerical simulation of rock breaking by PDC cutters in hot dry rocks," *Natur. Gas Ind.*, vol. 39, no. 4, pp. 125-134, Apr. 25, 2019.

[12] Xu Peng, Shijun Hao, "Rock breaking mechanism of composite impact of full-size PDC bit based on finite element analysis," *Coal Geology & Exploration*, vol. 49, no. 2, pp. 240-246, 2021. doi: 10.3969/j.issn.1001-1986.2021.02.030

[13] M. He, B. Huang, C. Zhu et al., "Energy dissipation-based method for fatigue life prediction of rock salt," *Rock Mechanics and Rock Engineering*, vol. 51, no. 5, pp. 1447-1455, 2018.